AD 653027

COPY NO. 18

TECHNICAL REPORT 3555

THE WATER ADSORPTION PROPERTIES OF THE POLYMORPHS OF HMX: THE THERMODYNAMICS OF WATER INTERACTION WITH GROUND AND UNGROUND BETA-HMX

THOMAS C. CASTORINA

JEROME HABERMAN

MAY 1967

D D C
RECEIVED
JUN 14 1967
B

DISTRIBUTION OF THIS DOCUMENT IS UNLIMITED

PICATINNY ARSENAL
DOVER, NEW JERSEY

ARCHIVE COPY

39

Technical Report 3555

THE WATER ADSORPTION PROPERTIES OF THE POLYMORPHS OF HMX: THE THERMODYNAMICS OF WATER INTERACTION WITH GROUND AND UNGROUND BETA-HMX

by

Thomas C. Castorina
Jerome Haberman

May 1967

Distribution of this document is unlimited

AMCMS Code 5016.11.844
Dept of the Army Project 1L013001A91A

Explosives Laboratory
Feltman Research Laboratories
Picatinny Arsenal
Dover, N. J.

TABLE OF CONTENTS

	Page
Abstract	1
Introduction	2
Experimental	3
Preparation of Adsorbents	3
Adsorbates	4
Adsorption Measurements	4
Calculations of Thermodynamics of Water Adsorption	5
Discussion	9
Results	10
Conclusions	13
References	14
Distribution List	32

Figures

1	Specific volume adsorption of H_2O on polymorphs of HMX at 25° vs partial pressure	16
2	Adsorption isotherms of water on unground and ground β-HMX at 25°	17
3	Specific volume of water adsorption on ground and unground β-HMX at 25° as a function of partial pressure	18
4	Adsorption isotherms of water on ground β-HMX at 25° and 35°	19
5	Adsorption isotherms of water on unground β-HMX at 25° and 35°	20
6	Gibbs adsorption isotherms of water on unground β-HMX at 25° and 35°	21
7	Gibbs adsorption isotherms of water on ground β-HMX at 25° and 35°	22
8	Variation of free surface energy of unground β-HMX by water at 25° and 35° vs pressure	23

Page

Figures

9	Variation of free surface energy of ground β-HMX by H_2O at 25° and 35° vs pressure	24
10	Lowering of free surface energy of ground and unground β-HMX by H_2O at 25° as a function of specific volume adsorbed	25
11	Isosteric and integral heats of water on ground β-HMX vs specific volume of adsorption	26
12	Isosteric and integral heats of water on unground β-HMX vs specific volume of adsorption	27
13	Differential and integral entropy changes of water on unground β-HMX vs specific volume of adsorption	28
14	Differential and integral entropy changes of water on ground β-HMX vs specific volume of adsorption	29
15	Differential and integral entropies of water on unground β-HMX vs specific volume of adsorption	30
16	Differential and integral entropies of water on ground β-HMX vs specific volume of adsorption	31
17	Fisher model of a unit cell of β-HMX showing free and methylene-shielded NO_2 groups	32

ABSTRACT

Water adsorption isotherms were measured for the polymorphs of octahydro-1,3,5,7-tetranitro-s-tetrazine (HMX). Water is found to sorb into the crystal structure in the order, gamma-HMX > alpha-HMX, and not at all into beta-HMX. The thermodynamics of water interaction with the surface of beta-HMX was studied as a function of grinding action. Grinding reduces the free surface energy of beta-HMX from 25 to 5 ergs/sq cm, and increases the hydrophobic character of the surface by a factor of 12. The calculated thermodynamic functions support the concept of adsorption of water in clusters on both ground and unground beta-HMX surfaces. The integral heat of water adsorption increases with increasing hydrophobicity. This is attributed to unhindered dipole interaction of water with the more isolated active sites of like charges. Accordingly, water is shown to become less entropic as the hydrophobicity is increased.

INTRODUCTION

In the simplest case of a body-centered cubic crystal composed of like atoms the 001, 011, and 111 faces will possess different surface properties due to differences in the packing densities of the atoms on the respective faces. Markedly accentuated surface heterogeneities are characteristic of crystals composed of organic molecules by virtue of variations in the spatial arrangements of polar functional groups along the crystallographic faces.

Experimental evidence shows (Ref 1) that hydrophilic (polar) heterogeneities are responsible for the adsorption of water. Surfaces which are homopolar, or nearly so, and exhibit practically no electrostatic force field, are found experimentally to be hydrophobic and give rise to Type III isotherm behavior with water. In these cases there is no contribution to adsorption forces from dipole attractions or polarization of the adsorbate, and the only major attraction arises from dispersion forces. Dispersion forces alone are not sufficient to give rise to a normal monolayer coverage with subsequent multilayer formation, in the case of water vapor at room temperature on homopolar surfaces.

Physical adsorption of water vapor could be restricted to the vicinity of polar sites even at relatively high pressures. Adsorption is initiated on the surface polar site and probably proceeds by building up clusters of adsorbed molecules around these sites via mutual interactions of the water dipoles. Thus, even at pressures approaching saturation, those portions of the surface that are devoid of heteropolar characteristics would be bare of adsorbed water molecules. This is supported by the fact that in such cases sufficient water vapor for complete monolayer coverage cannot be adsorbed, even at relative pressures close to saturation on surfaces with few polar sites. For such heterogeneous surfaces, the isotherms obtained are predominantly Type III, except for an initial rise in the curves, suggestive of Type II, which is attributed to adsorption at the relatively few hydrophilic sites.

On the assumption that the water adsorbs only on hydrophilic or polar sites, the ratio of the volume of water adsorbed at monolayer coverage to the surface area of the substrate can be used to characterize the heterogeneity of surfaces before and after various treatments. The surface may be characterized further by determining thermodynamic functions such as free surface energies, and enthalpies and entropies of water adsorption. Isosteric heats calculated from the water adsorption isotherms could indicate if the hydrophilic sites are of equal energies. Entropies derived from the heats of adsorption may give some insight into the mobility of the adsorbed surface film.

Surface heterogeneities may play a critical role in the observed properties of materials. For example, though little of the surface is covered by adsorbed water molecules, the presence of these few molecules is sufficient to prevent the rapid wear of carbon brushes in electric motors and to allow the use of graphite as a lubricant.

Because of their presumably high degree of surface heterogeneity, and in some cases open structure, organic explosives are expected to exhibit relatively strong interaction with water. Since water vapor is the major constituent adsorbed at ambient temperature from the atmosphere to which these explosives are exposed, the relationship of the presence of this water to the bulk properties could be of significant importance. Accordingly, a study was undertaken to determine the water adsorption properties of octahydro-1,3,5,7-tetranitro-s-tetrazine (HMX). HMX exists in four polymorphic configurations, HMX-I(β), -II(α), -III(γ), and -IV(δ), with densities ranging from 1.96 to 1.78 (Ref 1) . As such, this explosive is most suitable for the study of water interaction as a function of polymorphism before and after various treatments and as a function of density or degree of open structure.

EXPERIMENTAL

Preparation of Adsorbents

All sample aliquots were obtained from a master batch of beta-HMX purified by successive recrystallizations from acetone (Ref 2). The particle sizes cited below were obtained from surface areas, Σ, determined by argon adsorption on the assumption that the HMX particles are spheres with smooth surfaces (Ref 3). In this case

$$d = \frac{6}{\rho\Sigma} \tag{1}$$

where Σ is the specific surface in sq cm of the adsorbent, ρ is its density, and d is the average particle diameter.

Fine-particle-size HMX-I(β) of 21 microns diameter ($\Sigma = 0.15\ m^2/g$) was prepared by adding a solution of 5 g HMX in 48 cc dimethylsulfoxide (DMSO) to a mixture of 120 cc absolute ethanol and 6 cc acetone. The precipitate was stirred 10 minutes, filtered, washed with absolute ethanol, and air dried.

Ultrafine-particle-size (powder) HMX-I(β) of 1 micron diameter (Σ = 2.8 m^2/g) was prepared by grinding beta-HMX with mortar and pestle.

Fine-particle-size HMX-III(γ) of 16 microns diameter (Σ = 0.2 m^2/g) was prepared by recrystallization from 50% aqueous acetic acid as described in Reference 4.

Ultrafine-particle-size (powder) HMX-III(γ) of 1 micron diameter (Σ = 2.8 m^2/g) was prepared by adding a 1:4 solution of HMX:DMSO to rapidly agitated cold water. The volumes of solution and precipitation medium were in the ratio of 1:10. The precipitate was filtered rapidly, washed with small portions of cold water, and spread on filter paper to air-dry.

In all cases the identity of the polymorphs was made by infrared and checked by X-ray analysis. The crystalline character of fine particle gamma, and ground beta-HMX was established by X-ray analysis.

Adsorbates

Water: Distilled water was redistilled from alkaline permanganate and sulfuric acid, followed by a third redistillation. The water was finally degassed by freeze-thawing under vacuum.

Gases: Nitrogen, helium, krypton, and argon were of high purity Baker's reagent grade.

Adsorption Measurements

In preparation for adsorption measurements, fine and ultrafine beta-HMX required 24 hours, and gamma-HMX powder 4 weeks, of outgassing at ambient temperatures. The completion of outgassing was checked by observing any pressure rise in a closed system at the end of a two-hour interval.

Nitrogen and argon adsorption measurements at −195° were made with a Brunauer-Emmett-Teller (BET) type apparatus. Krypton was used as the adsorbate for small area samples, and equilibrium pressure readings were made with a Pirani gauge calibrated for krypton. For calculations of surface areas, the linear form of the BET isotherm equation for multi-layer physical adsorption of a free surface was used (Ref 5):

$$\frac{p}{v(p_o - p)} = \frac{1}{v_m c} + \frac{(c-1)}{v_m c} \cdot \frac{p}{p_o} \qquad (2)$$

where v_m is the monolayer capacity, i.e., the volume of gas adsorbed when the entire surface of adsorbent is covered with a complete unimolecular layer, p is the equilibrium pressure, and p_o is the vapor pressure of the gas at temperature T; $c = c_0 \exp (E_1 - E_L)/RT$ or $\ln c = -(E_1 - E_L)/RT + \ln c_0$, where E_1 is the average heat of adsorption of the first layer, and E_L is the latent heat of condensation of the vapor. When a BET surface area plot is made of $p/v(p_o - p)$ versus p/p_o, a straight line is obtained from 0.05 to approximately 0.30. The monolayer capacity, v_m, is obtained from the intercept, $1/v_m c$, and the slope, $(c - 1)/v_m c$. Finally, from the v_m value Σ was calculated, using the assigned nitrogen, argon, and krypton adsorbate areas of 16.2, 14.6, and 19.6 A^2, respectively. The surface areas from BET plots of Ar, N_2, and Kr corresponded to values obtained by the B point method (Ref 3) within the limits of experimental error. The quantity v_m for water adsorption was determined by the B point method.

Water adsorption measurements were made with a modified Orr apparatus (Ref 6), adjusted with an Apiezon B oil-filled manometer. In the sorption experiments on gamma-HMX, equilibrium pressures were based on three successive readings of constant value within one hour. To obtain a sorption point, approximately three hours were required. With beta-HMX, however, equilibrium pressures were reached in less than ten minutes, although actual readings were recorded at the end of one hour.

All of the observed adsorptions were found to be completely reversible. The adsorption isotherm of water on the glass of the sample system was within the experimental error involved in the adsorption measurements and was therefore ignored.

Calculations of Thermodynamics of Water Adsorption

Isosteric (or differential) heats of adsorption, $H_G - \bar{H}_S$, of water on beta-HMX were calculated in the usual manner from the integrated form of the Clausius-Clapeyron equation at constant volume, v.

$$q_{st} = (\partial \ln p/\partial T)_v = (H_G - \bar{H}_S)/RT^2 \tag{3}$$

$$q_{st} = \frac{R(\ln P_2 - \ln P_1)}{(1/T_1 - 1/T_2)} = (H_G - \bar{H}_S) \tag{4}$$

where subscripts G and S denote gas phase and adsorbed state of water, respectively.

The total or integral heat of adsorption $(H_G - H_S)$ was obtained from the Clausius-Clapeyron equation as above, but at constant film pressure, π. The quantity π is by definition the free surface energy (Ref 7). It was therefore necessary to determine the free surface energy of adsorption as a function of spreading pressure at two different temperatures (Figs 4 and 5) by the Gibbs adsorption isotherm equation as first shown by Bangham (Ref 8):

$$\pi = RT/V\sigma \int_{p=0}^{p=p_o} v/p \, dp \tag{5}$$

where V is the molar gas volume, σ is the area for one gram of solid, v is the volume of adsorbed gas per m^2 of surface, p is the equilibrium pressure of adsorbing gas, and p_o is the vapor pressure of the gas at temperature T. Graphical integration of the Gibbs isotherm (a plot of v/p versus p; Figures 6 and 7, pp 21 and 22) from zero pressure to saturation pressure gives the decrease in the change of the free surface energy of adsorption. The total reduction in free surface energy of the solid resulting from the adsorbate in equilibrium with the liquid adsorbate is often referred to as the equilibrium spreading pressure (Ref 9) of the adsorbed film. The lengthy calculations were FORTRAN programmed on an IBM 360 computer by the Scientific and Engineering Applications Division, DPSO at Picatinny Arsenal.

The differential and integral entropies of adsorption are given by the equation (Ref 10):

$$(S_S - S_L^{\circ}) = (S_S - S_G) + \Lambda/T - R\ln X \tag{6}$$

where X is p/p_o, Λ is the heat of liquefaction of water (10.5 kcal/mole), S_L° is the standard state of liquid water (16.7 e.u.), and S_S is the entropy of water in the adsorbed state, assuming an unperturbed adsorbent.

The term $(S_S - S_G)$ is derived from the respective differential and integral enthalpies, e.g., in the case of the differential enthalpies:

$$q_\theta = (\partial \ln p/\partial T)_\theta = (H_G - \bar{H}_S)/RT^2 = (S_G - \bar{S}_S)/RT \tag{7}$$

$$S_G - \bar{S}_S = (H_G - \bar{H}_S)/T \tag{8}$$

RESULTS

Large-particle gamma- and alpha-HMX could not be degassed completely of occluded solvents, even at temperatures as high as 110° under vacuum. Continued degassing under these conditions resulted in incipient decomposition, as indicated by mass spectral analysis. The sorption points, which required a minimum of 16 hours for equilibrium pressures to be attained, were determined from both partially degassed samples. These points, which are plotted in Figure 1 (p 16), show that water sorbs into the crystal structure. The action of grinding these samples resulted in conversions to mixtures of polymorphs. Because of these complications and impractical time factors involved in degassing and attaining equilibrium pressures, no further work was done with fine-particle alpha- and gamma-HMX.

The isotherm for the sorption of water into ultrafine-particle gamma-HMX, shown in Figure 1, is Type I, characteristic of adsorbents with open structure a few molecular diameters in width (Ref 11). Water sorbs into the gamma-HMX crystal in a ratio of one mole of water to 6.8 moles of HMX, and at saturation to the extent of 13 mole percent. The interaction of water with ultrafine-particle (ground) and fine-particle (unground) beta-HMX is demonstrated below to be confined to the surface.

The isotherms for the adsorption of water on unground and ground beta-HMX (hereafter referred to as ug- and g-HMX, beta form understood) are plotted on a specific area basis in Figure 2 (p 17) for BET calculations and on a specific volume basis in Figure 3 (p 18) primarily for purposes of comparison. The amounts of water adsorbed at monolayer coverage, v_m, estimated by the B point method from an expanded lower pressure region of Figure 2, are 5.5 and 8.0 $\times 10^{-3}$ cc/g for the ug- and g-HMX. Although grinding produces a 20-fold increase in surface area, it results in only a 1.5-fold increase in the amount of water adsorbed. In terms of specific volume of water adsorbed at monolayer coverage, v_m/m^2, as shown in Figure 3, the small quantity of 3.7×10^{-2} cc/m^2 is further reduced by grinding to 3.0×10^{-3} cc/m^2, or by a factor of 12. This increased hydrophobicity induced by grinding is observed even at relatively high p/p_o (0.7). The nonporosity of beta-HMX to water is further demonstrated by the 10-minute periods required to attain equilibrium pressures and by the complete desorptions achieved within an hour after exposure to vacuum. Although both isotherms are basically Type III, that of ug-HMX has a larger knee than that of the g-HMX. This may be attributed simply to the difference in magnitude of the specific volume of water adsorbed in the low p/p_o region.

Adsorption isotherms of water on g- and ug-HMX at 25° and 35° are shown in Figures 4 and 5 (pp 19 and 20). Extensive experimental determinations of specific volumes of adsorbed water are plotted over the lower pressure region of the

isotherms, from 0.006 to 0.3 p/p_o, for calculating differential and integral heats of adsorption at constant coverage and film pressure, respectively.

Plots of these data in terms of a Gibbs adsorption isotherm, p/v versus p, for the respective samples are shown in Figures 6 and 7 (pp 21 and 22). The shape of each curve depends on the shape of the corresponding isotherm produced in Figures 2 and 3. The area beneath the curve is integrated along the abscissa; the greater the displacement of the curve from the abscissa, the greater is the lowering of the free surface energy. For any particular sample of HMX the change in the free surface energy by the adsorption of water is shown to increase as the temperature is decreased.

When the free surface energy is normalized in terms of ergs cm^{-2} (π), and plotted versus pressure, as in Figures 8 and 9 (pp 23 and 24), the integral heats of adsorption can be calculated from the Clausius-Clapeyron equation at constant π. The data presented in this form also make possible comparison of π's of different samples by the adsorbate. Thus, comparison of Figures 8 and 9 shows that the lowering of free surface energy by water adsorption decreases with grinding by one order of magnitude.

The relationship of free surface energy to specific volume of water adsorbed for both samples of HMX is shown in Figure 10 (p 25). The absence of two points of inflection in the curve for the ug-HMX is indicative of a nonporous solid (Ref 7). Because of the high degree of hydrophobicity (~99%), the curve for the g-HMX could not be extended beyond the specific volume of 0.04 cc/m^2. Despite this limitation, the deviation from the curve for ug-HMX is considered real (see Figures 8 and 9). The lowering of the free surface energy is shown to be, not only a function of the total amount of water adsorbed, but, at a fixed specific volume, an intrinsic function of the sample substrate. The lower limit of pressure that can be read with reasonable accuracy on the oil manometer is equivalent to 0.01 cc/2 g sample (sizes larger than 2 g require excessively long periods of time for the equilibration of pressures). Since the cc/g is a product of a specific volume and specific area, the lowest readable specific volume for the g-HMX (2.8 m^2/g) was 0.003 cc/m^2 and for the ug-HMX (0.15 m^2/g) was 0.03 cc/m^2. Due to this limitation, all subsequent curves are not shown to extend to values below the region of 0.03 cc/m^2.

The isosteric (differential) and integral heat values calculated from the isothermal data at two temperatures are plotted as a function of the specific volume of adsorbed water in Figures 11 and 12 (pp 26 and 27). The error limits of the calculated points of these and all subsequent figures represent the maximum probable error as estimated from the maximum deviations of the isothermal adsorption values.

The distribution and magnitude of the differential heats ($H_G - H_S$) of ug- and g-HMX are very similar and are in agreement with their respective v_m and statistical monolayer coverages. However, the integral heats ($H_G - H_S$) of ug-HMX are shown to lie well below the heat of liquefaction of water (H_L), whereas those of the g-HMX fall at the H_L level. This apparent difference is consistent with the observed differences in the lowering of the free surface energy.

The differential and integral entropy changes of water on g- and ug-HMX are plotted versus specific volume of water adsorbed in Figures 13 and 14 (pp 28 and 29). At v_m the maxima and minima are in agreement with the minima and maxima of the corresponding heats of adsorption. The absolute entropies of water in the adsorbed state, as calculated by the relationship according to Hill (Ref 10; see section on calculations), are plotted as a function of the specific volume of water adsorption in Figures 15 and 16. In conformity with the heats of adsorption, the S_S of water decreases considerably with grinding. The minimum in the S_S curve in Figure 16 has been cited by Hill (Ref 12) as a thermodynamic criterion for the completion of the monolayer coverage, v_m. The minimum in the S_S curve in Figure 15 (p 30) is not shown for the reason given above. The differential and integral entropies of water in the adsorbed state on g- and ug-HMX lie well above the entropy of liquid water, S_L, in the standard state.

DISCUSSION

When the Σ covered by an adsorbate in a Type I isotherm is much greater than the N_2 and/or Ar Σ's which are in agreement with the geometric Σ, the adsorbate is said to be sorbed into the adsorbent structure, where the molecular diameter of the adsorbate is necessarily smaller than that of either N_2 or Ar. In the case of water interaction with open-structured crystals, sorption at ambient temperatures can only take place with internal surfaces that are polar in nature. The polymorphs of HMX seem to satisfy the conditions for the sorption of water by virtue of their allegedly open structure and polar internal surfaces (Ref 4). The extent to which water sorbs into the crystal structure of the polymorphs decreases in the order of increasing density: gamma-HMX (d = 1.76) > alpha-HMX (d = 1.82) and not at all into beta-HMX (d = 1.93). Apparently, the open structure of gamma- and alpha-HMX is sufficiently large to accommodate water (diam. = 3.68 A) and not Ar (diam. = 4.24 A). The sorption of water into these polymorphs showed no indication of being dependent upon particle size, at least to the extent the investigation was carried out.

Delta-HMX was not included in this study because it transforms readily to a mixture of beta and gamma forms. With the exception of gamma-HMX, the preparation of powders by precipitation methods was not possible. In each case a mixture of the polymorphs was obtained.

Because of the difficulties encountered in the preparation of samples in widely varied particle size, the original plan to study the thermodynamics of water adsorption by the polymorphs of HMX as a function of particle size was abandoned. The only polymorph that was prepared in two widely different particle sizes, subject to such a study, was beta-HMX. But this could only be accomplished mechanically, thereby introducing the added variable of the effect of grinding action on the surface of the crystalline substrate.

In this case, the factor of particle size effect is not favored, based on the general theory of solids, substantiated by electron photomicrographs which indicate that fine crystals (< 40 microns) do not exhibit cracks such as may be found in large crystals (Ref 13). The fine-particle beta-HMX crystals (~ 20 microns) and ultrafine beta-HMX powder (~ 1 micron) which was shown by X-ray analysis to be crystalline in character would not be expected to show any differences in the crystalline order of their surfaces based solely on particle size in this low range. Therefore, any difference in surface structure of these samples would be due predominantly to the action of grinding by which the ultrafine crystalline powder is formed. Grinding could conceivably result in a disturbed layer, cracks, or reduced crystalline order at the surface of the subdivided particles.

A Fisher model of a unit cell of beta-HMX is shown in Figure 17 (p 31). The ends have freely exposed hydrophilic nitro groups, whereas the nitro groups in the lateral planes are somewhat shielded by methylene hydrogens. One can consider the electrostatic force field of attraction exerted by the nitro oxygens to be reduced by the methylene hydrogens in close proximity, and therefore to present a hydrophobic plane. In the multiple stackings of the unit cell even the terminal nitro groups fall in the shielded pattern. This would explain the essentially hydrophobic character of beta-HMX. Consistent with this interpretation is the fact that the change in free surface energy of beta-HMX by the adsorption of water is approximately 25 ergs/cm^2. As such, beta-HMX is accurately described as possessing a low-energy surface. Therefore, the limited quantity of water that is adsorbed presumably can take place only at sites where the nitro oxygens are freely exposed at crevices, edges, or cracks on the surface. Grinding is shown to increase these exposures only by a factor of 1.5 with a concurrent 20-fold increase in surface area.

Thus, in the ensuing discussion the observed differences in the thermodynamics of water adsorption by the surfaces of these two samples of beta-HMX are attributed to the grinding action alone and the appropriate differentiation is made, g- and ug-HMX.

The adsorption of water vapor is restricted to polar sites and not to homopolar areas of uniform energies (Ref 9). Surfaces which are, in the major part, homopolar exhibit very little electrostatic force field and are found experimentally to be hydrophobic, giving rise to Type III isotherm behavior with water. Since the isotherms shown in Figure 3 have predominant Type III character except for the slight rise in the curves at low p/p_o suggestive of Type II behavior, the surfaces of both g- and ug-HMX are demonstrated to be heterogeneous. The initial rise is attributed to the adsorption of water at the hydrophilic sites (strong adsorbate-adsorbent interaction). As postulated by Pierce and Smith (Ref 14), after adsorption of the first layer of water molecules on these sites, additional layers are formed on and around the already adsorbed molecules rather than on the neighboring hydrophobic area (weak to no adsorbate-adsorbent, but strong adsorbate-adsorbate interactions). The broad deviations of the respective fractions of water coverages from complete coverage of the available areas of g- and ug-HMX, 0.007 and 0.11 (at v_m); 0.11 and 0.46 (at $p/p_o = 0.35$ where multilayer adsorption usually takes place), would indicate clustering of adsorbed water molecules in the vicinity of polar sites. This is further illustrated at relatively high pressures. In the case of g-HMX, at a maximum attainable $p/p_o = 0.78$, only 0.65 of the statistical monolayer is adsorbed. For ug-HMX slightly more than one statistical monolayer is adsorbed at $p/p_o = 0.99$. In going from ug-HMX to g-HMX, as the number of hydrophilic sites decreases per unit area and the distance between them increases, the shape of the isotherm is shown to assume more Type III character. In comparison to the ug-HMX, this change of adsorbate interaction could be indicative of a more random scatter of active sites in addition to the reduction of their numbers induced by the grinding action.

The variations of π with temperature and pressure by the adsorption of water on g- and ug-HMX are as expected for heterogeneous surfaces. An initial sharp rise, followed by a monotonic increase in π-change with increasing pressure, is more pronounced at the lower temperature, However, the π of beta-HMX is markedly reduced by the grinding action, which increases the area of the particles from 0.15 to 2.8 m^2/g. On the basis of particle size alone, this observation is not in agreement with the relationship of π to Σ demonstrated for SiO_2 by Every (Ref 15). In the range of surface areas from 0.1 to 120 m^2/g, the π is shown to have a maximum value at $\Sigma = 3\text{-}4\ m^2/g$. The decreasing values of π are attributed to an increasingly amorphous character of the surface with decreasing particle size (increasing surface

area). In spite of the evidence of the crystalline form of the g-HMX given by X-ray analysis, the crystalline order at the surface might have been disturbed by local heating due to the grinding action. But, in view of the close relationship between π and hydrophilicity, as indicated by the five-fold decrease in π induced by grinding being equal to the decrease in hydrophilicity, the consideration of an aperiodic amorphous surface is discounted. The incipient difference in the slopes of the curves in Figure 10 (p 25) may be ascribed here again to the difference in degree of random scatter of the hydrophilic sites between the samples.

The accuracy of the calculated thermodynamic functions is limited by the precision, indicated as vertical bars. In spite of this limitation the complex curves generated do indicate qualitatively the change in heterogeneity of beta-HMX induced by grinding and the corresponding differences in the interaction of adsorbate molecules. Although the differential functions give a good insight into the distribution of the high energy sites, integral functions make possible more meaningful interpretations due to their relative insensitivity to the error limits involved.

The heat curves obtained for g- and ug-HMX are typical of heterogeneous surfaces. Adsorption is shown to take place initially at the more energetic sites (water-polar site interaction) and with continued adsorption at the less energetic sites of more uniform energies (water-water interaction). Since the water molecule has a permanent dipole moment, the surface field force of beta-HMX may line up the adsorbed dipoles in the same direction. With continued adsorption approaching v_m, the distance between the aligned dipoles decreases, and the repulsive forces presented to additional adsorbate molecules increases, thereby resulting in diminishing heats of adsorption. It would appear that for the ug-HMX/H_2O system the repulsive forces exceed those of dispersion at, or in the vicinity of, monolayer coverages, whereas the reverse is true for the g-HMX/H_2O system. The reason for this may be that the dipolar water molecules oriented in the same direction on the polar planes containing like charges (unshielded negative oxygens of the NO_2 groups), being greater in number per unit area, are more closely packed at v_m on ug-HMX than on g-HMX. This would explain the higher heat of adsorption of water on g-HMX than on ug-HMX.

The subsequent corresponding changes in the heats of adsorption can be attributed to the association of H_2O - H_2O molecules, as in condensation, approaching the heat of liquefaction of water, H_l (sometimes referred to as heat of capillary condensation). Certainly, highly polar molecules such as water are characterized by a strong tendency towards association. It is interesting to note further that the heat of adsorption of water of ug-HMX is well below H_L. The high H_L of water is due largely to the formation of hydrogen bonds. Since the opportunity for hydrogen

bonding is less at the first and even second layer coverages, adsorbate interaction is expectedly less than in the three-dimensional liquid phase. Because of the strong adsorbate-adsorbent interaction unimpaired by repulsive forces in the g-HMX/H_2O system, the heat of adsorption, ΔH_a, is higher than the H_L and clustering in isolated patches is readily attained, where $\Delta H_a = H_L$. The closer the ΔH_a is to H_L the greater is the probability of finding complete two-dimensional translation freedom of the adsorbate at the surface. At higher coverages the substrate of both samples has less effect on the differential and integral heats as all curves tend to converge.

The maxima and minima in the integral heats and entropies of adsorption are not uncommon (Ref 12). The minimum in the S_S curve for water on g-HMX is in very good agreement with the value of v_m calculated by the B point method. Both of these methods of arriving at the v_m value substantiate the probability of clustering since monolayer adsorption is shown to take place at a very small fraction of surface coverage, $\theta = 0.007$. The entropy of adsorbed vapor gives some indication of the extent to which molecules are capable of two-dimensional translation on the surface.

Of the two samples, the ug-HMX surface, which shows the greater decrease in π with adsorption, also shows the least order of adsorbed water. The integral entropy is well above the entropy of water in the liquid phase. This water, being highly entropic, is almost gaslike in mobility. In the vicinity of v_m, the entropy of the adsorbed water is, oddly enough, at a maximum for the reason cited above for the heat of adsorption being at a minimum, i.e., due to a strong repulsive force field.

At v_m coverage of g-HMX the water is indicated to be almost ice-like due to the postulated unhindered interaction with the isolated hydrophilic sites. With continued coverage confined to these isolated patches, the entropic nature of the adsorbed water becomes more liquid-like, although it is still considerably less mobile than it is in the case of ug-HMX.

CONCLUSIONS

Based on the thermodynamics of water adsorption, the surface properties of an organic secondary explosive have been characterized for the first time. The polar nature, the degree of heterogeneity, and distribution of energy sites of beta-HMX have been elucidated. In addition, the manner in which these surface properties change with grinding has been revealed.

Of the three polymorphs studied, only beta-HMX is shown to adsorb water at the surface. The water is adsorbed primarily in patches and at saturation levels the water becomes very gas-like in mobility on the surface. Grinding is observed to render the surface of beta-HMX essentially hydrophobic and concurrently to increase the distance between patches of less entropic water molecules adsorbed on the surface.

The implications drawn from this knowledge could possibly be of use to those who formulate explosive compositions. Certainly, if increased hydrophobicity were a desired quality, where perhaps interparticulate forces of attraction are to be decreased, or if a decrease in the wetting property of beta-HMX were preferred, then mere grinding would be the most effective manner in which to achieve these ends. If increased hydrophilicity (wetting) were a required property of the particulate surface of explosives, any change induced at the surface in this direction could be monitored qualitatively by means of the thermodynamics of water interaction.

REFERENCES

1. W. C. McCrone, *Anal. Chem. 22*, 1225 (1950)

2. T. C. Castorina, F. S. Holahan, R. J. Graybush, J. V. R. Kaufman, S. Helf, *J. Am. Chem. Soc. 82*, 1617 (1960)

3. S. Brunauer, *The Adsorption of Gases and Vapors* (University Press, 1943), pp 293 and 287

4. M. Bedard, H. Huber, J. L. Myers, G. F. Wright, *Can. J. Chem. 40*, 2278 (1962)

5. S. Brunauer, P. H. Emmett, E. Teller, *J. Am. Chem. Soc. 62*, 1723 (1940)

6. A. C. Zettlemoyer, G. J. Young, J. J. Chessick, F. H. Healey, *J. Phys. Chem. 57*, 649 (1953)

7. G. Jura, W. D. Harkins, *J. Am. Chem. Soc. 66*, 1356 (1944)

8. D. H. Bangham, *Trans. Faraday Soc. 33*, 805 (1932)

9. W. D. Harkins, *The Physical Chemistry of Surface Films*, Rheinhold, 1952, p 239

10. T. L. Hill, *J. Chem. Phys. 17*, 520 (1949)

11. S. J. Gregg, *The Surface Chemistry of Solids*, Rheinhold, 1961, p 33

12. T. J. Hill, P. H. Emmett, L. S. Joyner, *J. Am. Chem. Soc. 73*, 5105 (1951)

13. W. D. Harkins, G. Jura, *J. Am. Chem. Soc. 66*, 1362 (1944)

14. C. Pierce, R. N. Smith, *J. Phys. Chem. 54*, 795 (1950)

15. R. L. Every, W. H. Wade and N. Hackerman, *J. Phys. Chem. 65*, 25 (1961)

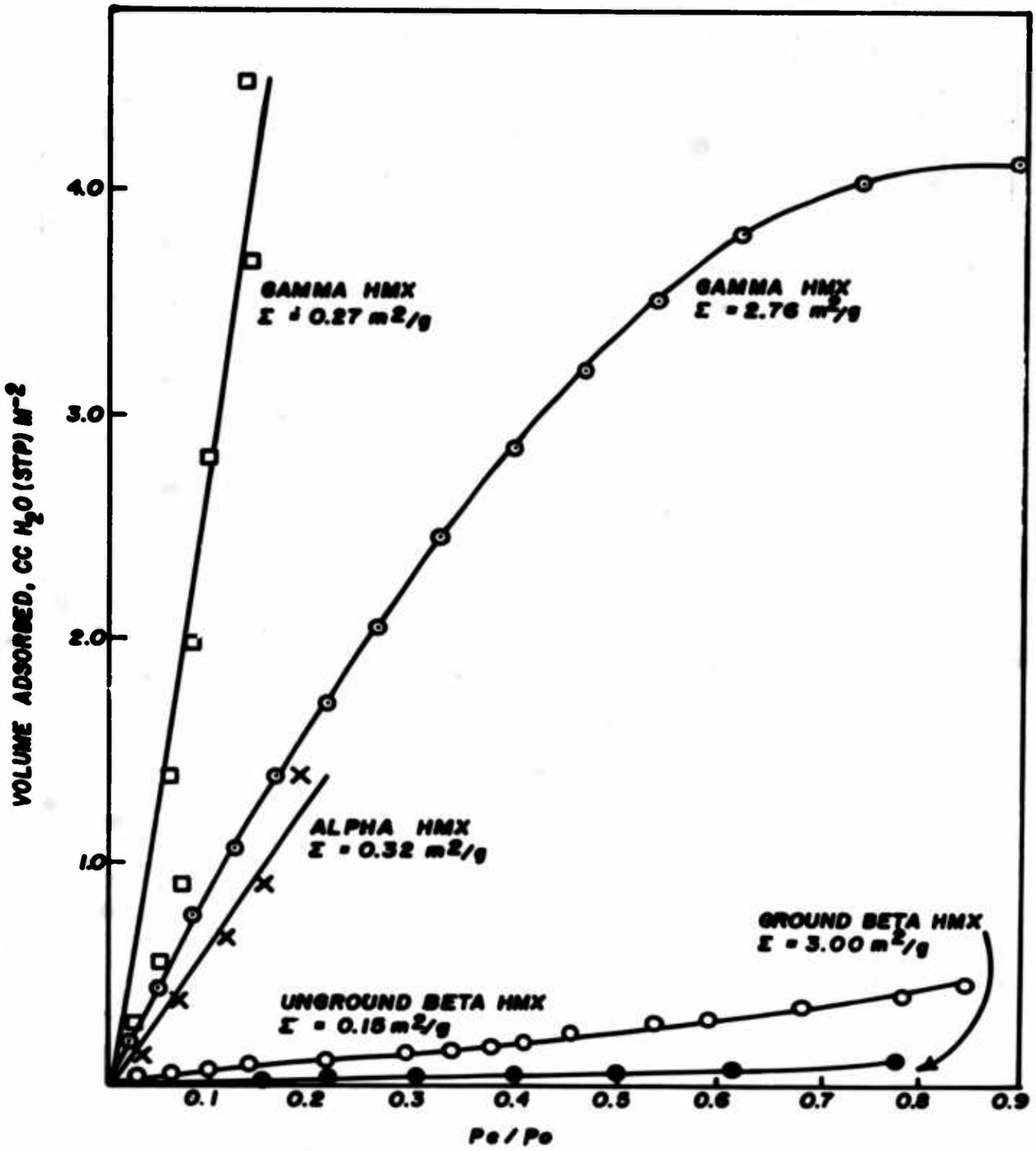

Fig 1 Specific volume adsorption of H_2O on polymorphs of HMX at 25° vs partial pressure

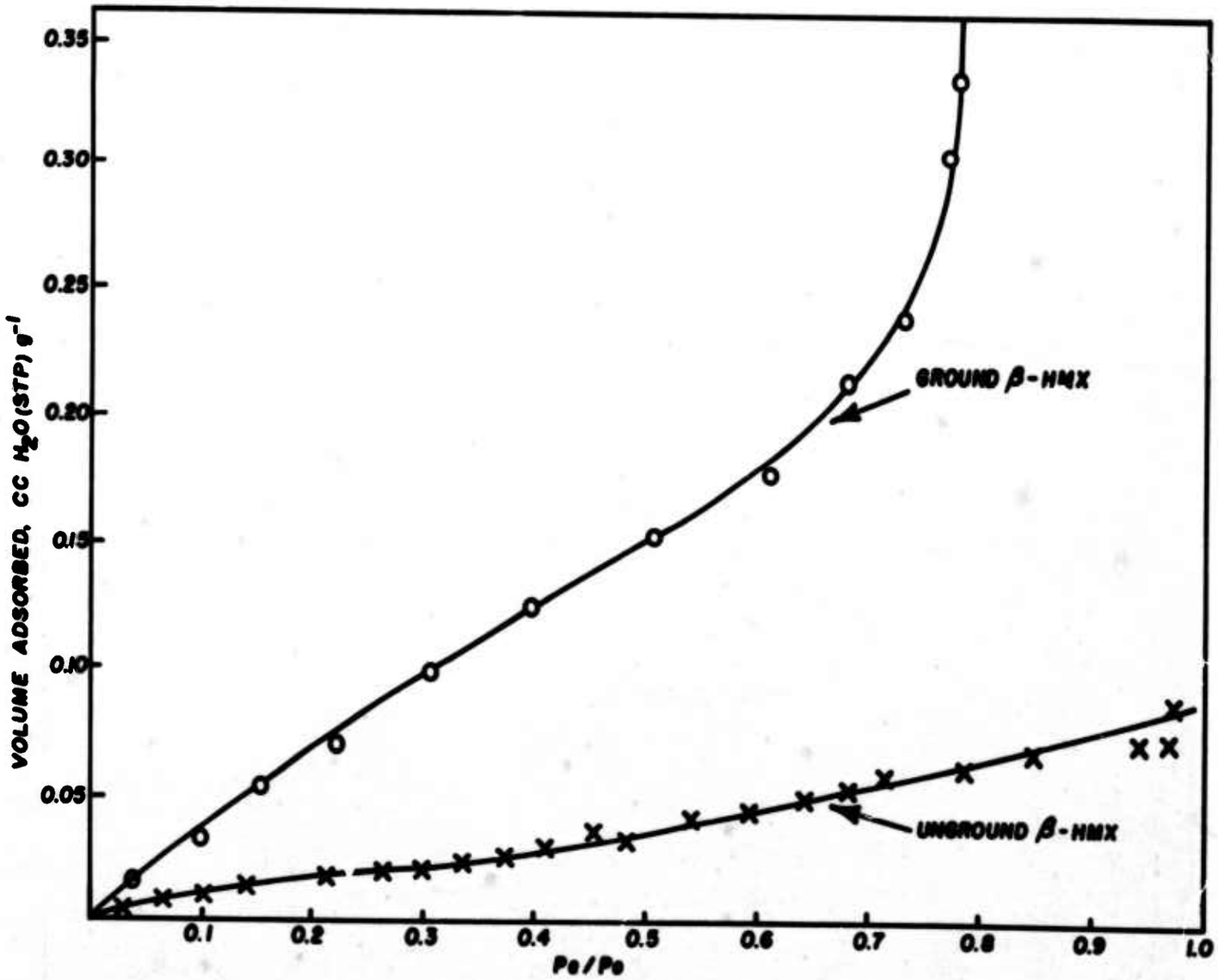

Fig 2 Adsorption isotherms of water on unground and ground β-HMX at 25°

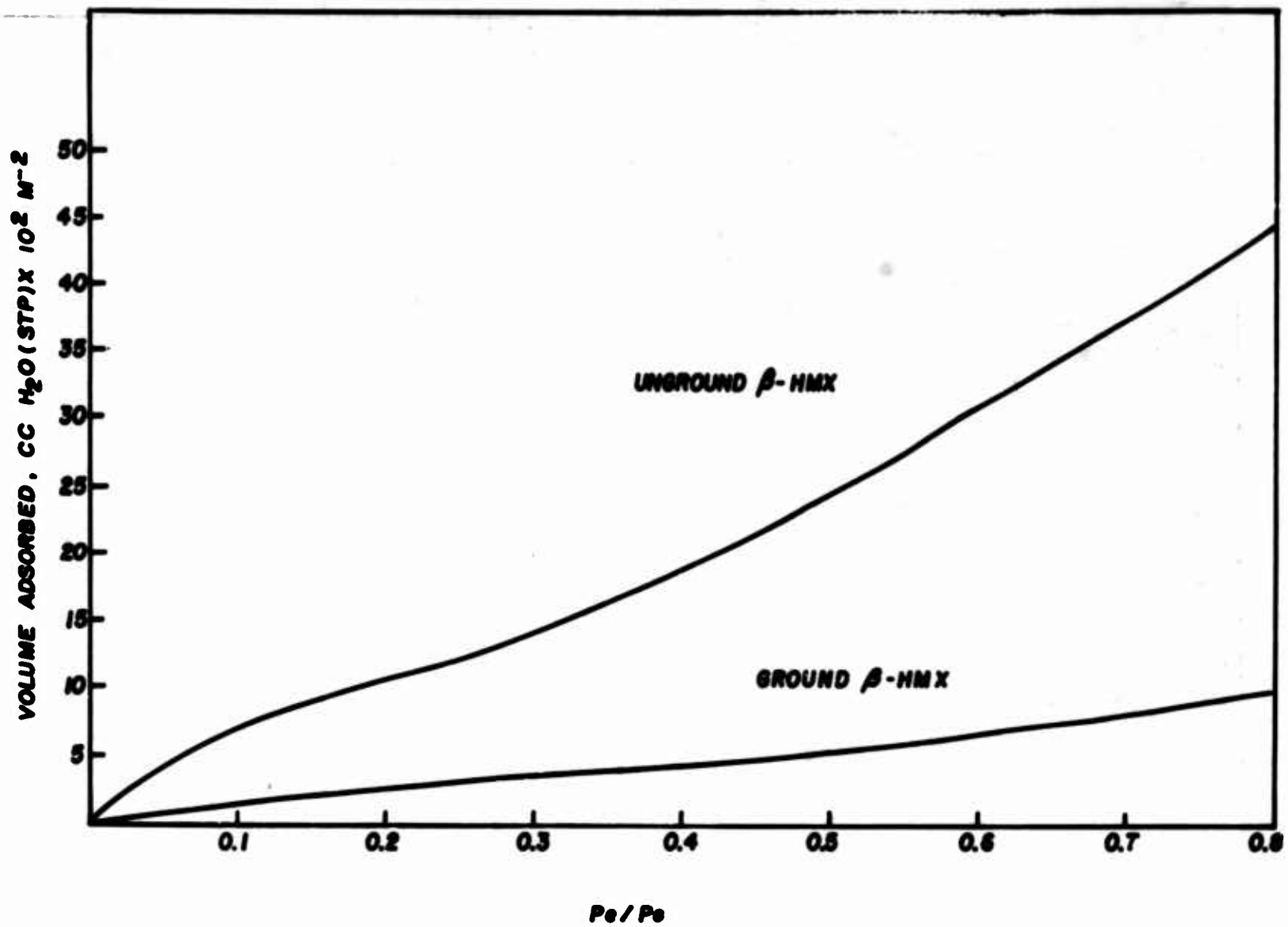

Fig 3 Specific volume of water adsorption on ground and unground β-HMX at 25° as a function of partial pressure

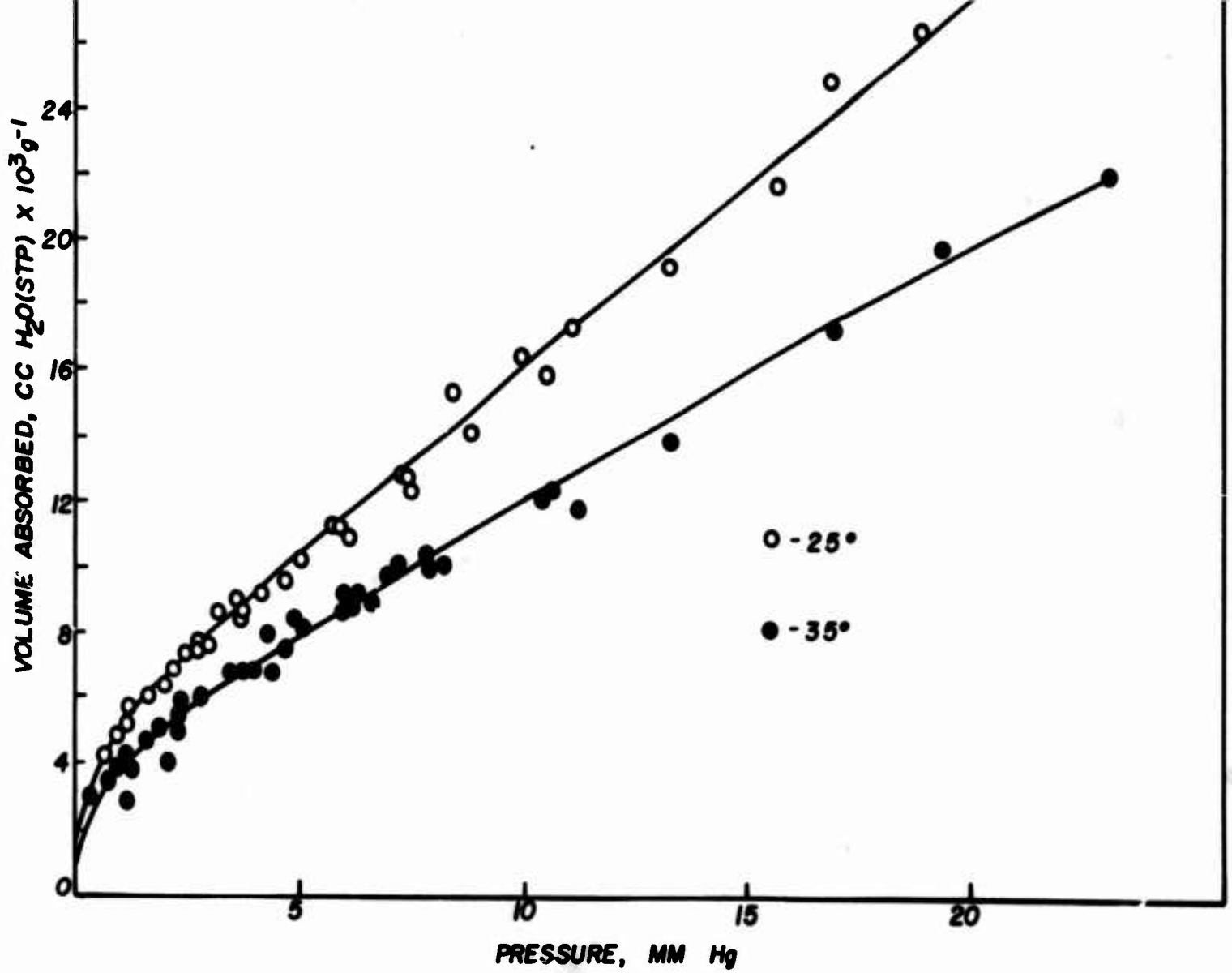

Fig 4 Adsorption isotherms of water on ground β-HMX at 25° and 35°

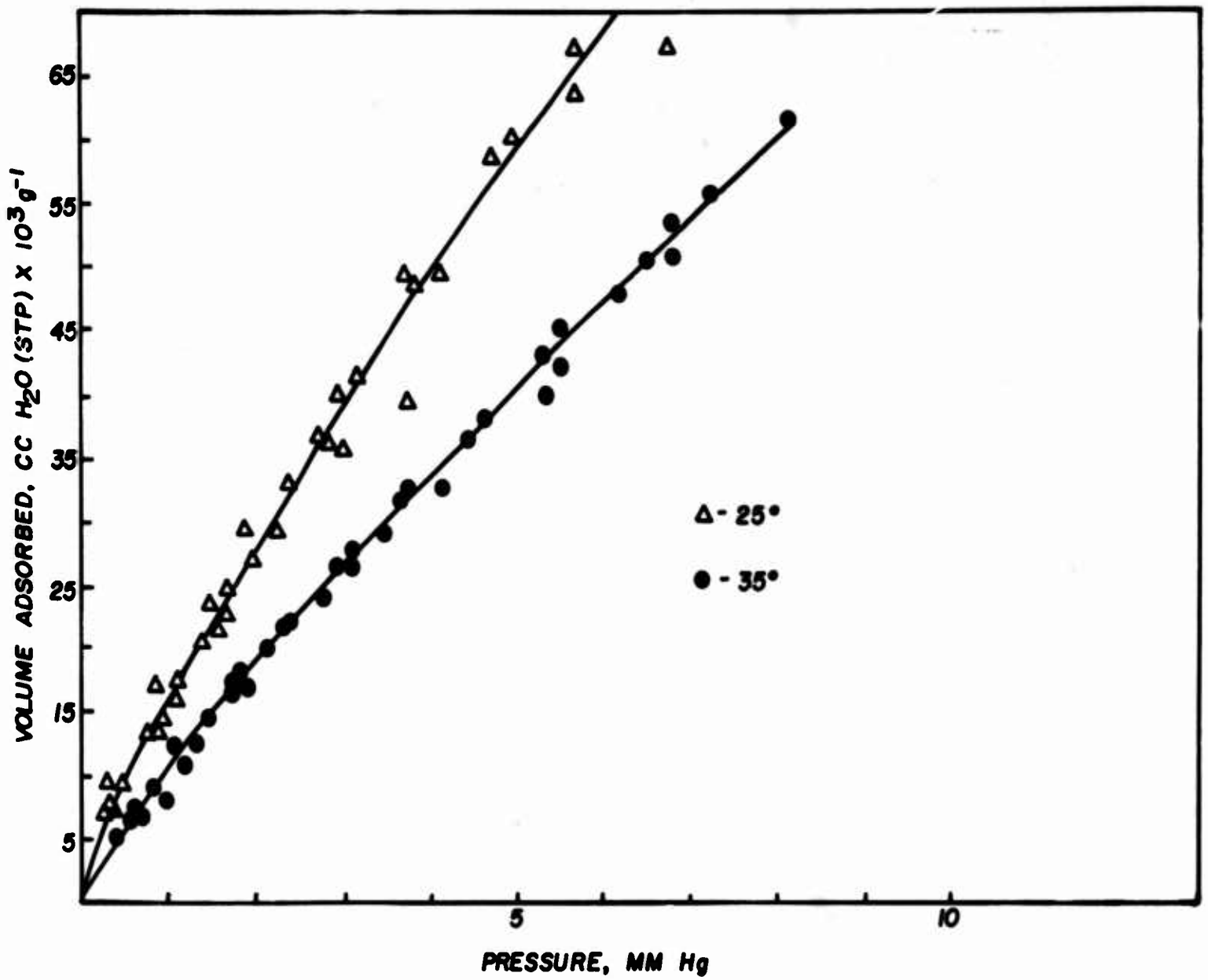

Fig 5 Adsorption isotherms of water on unground β-HMX at 25° and 35°

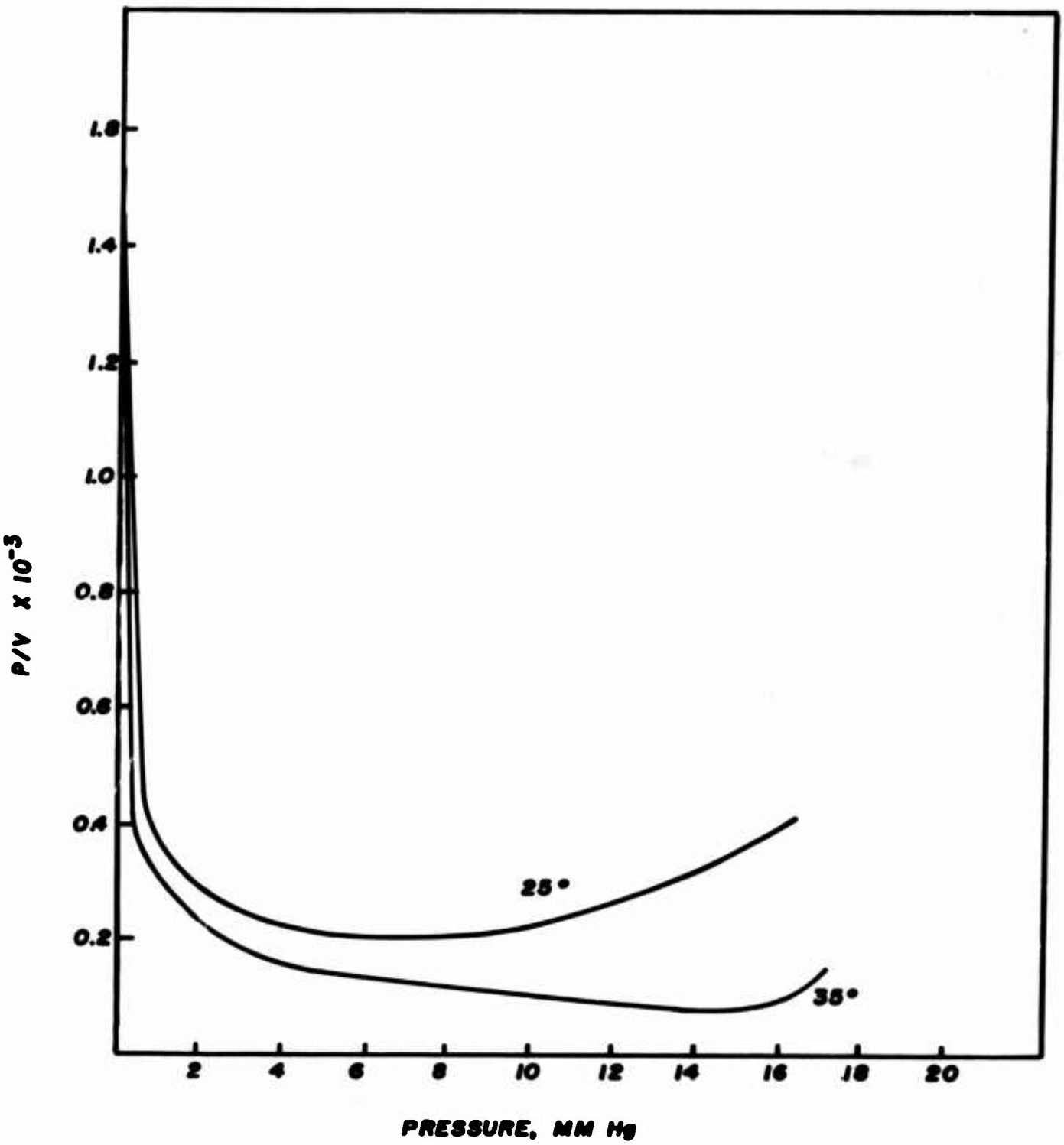

Fig 6 Gibbs adsorption isotherms of water on unground β-HMX at 25° and 35°

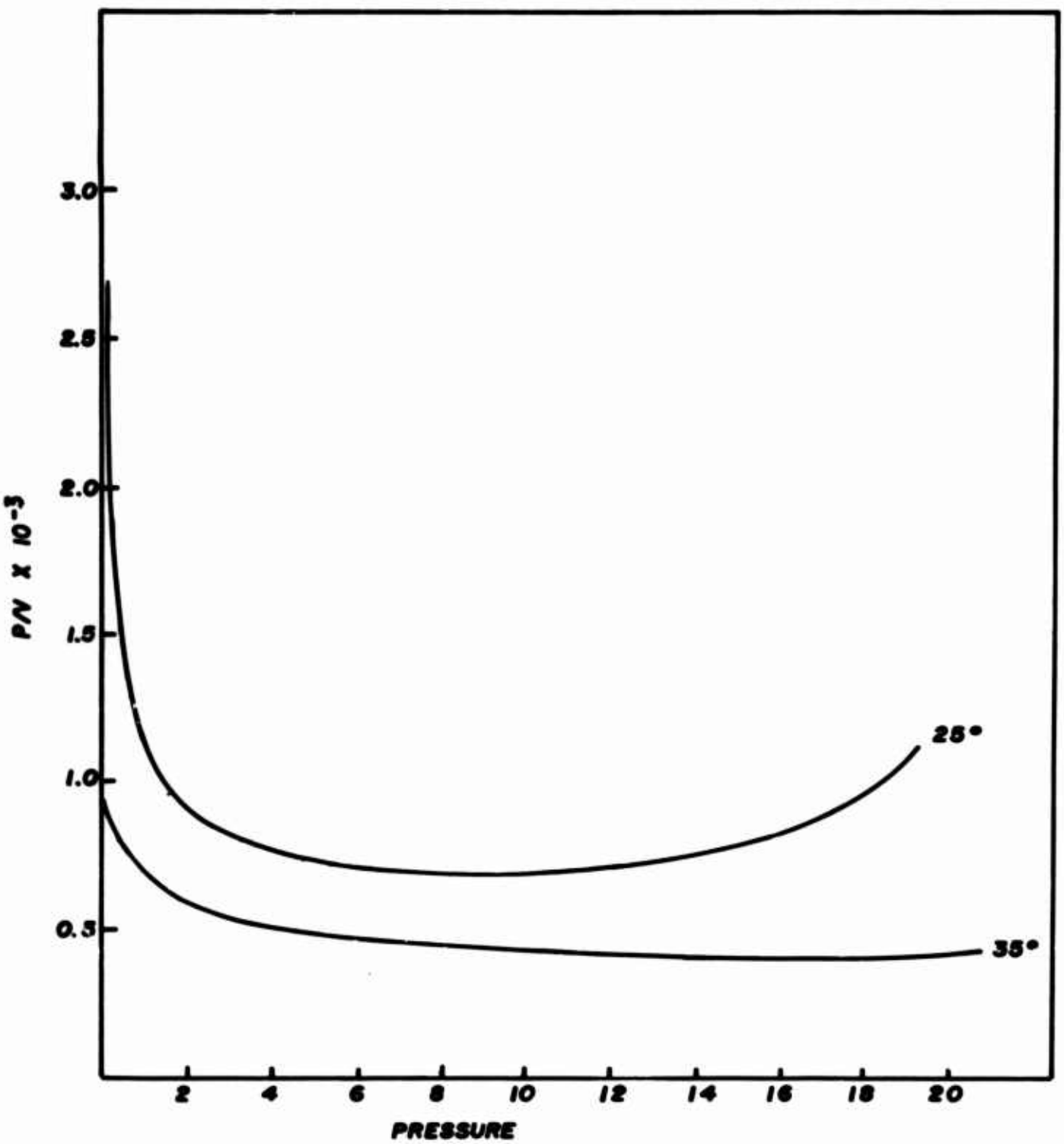

Fig 7 Gibbs adsorption isotherms of water on ground β-HMX at 25° and 35°

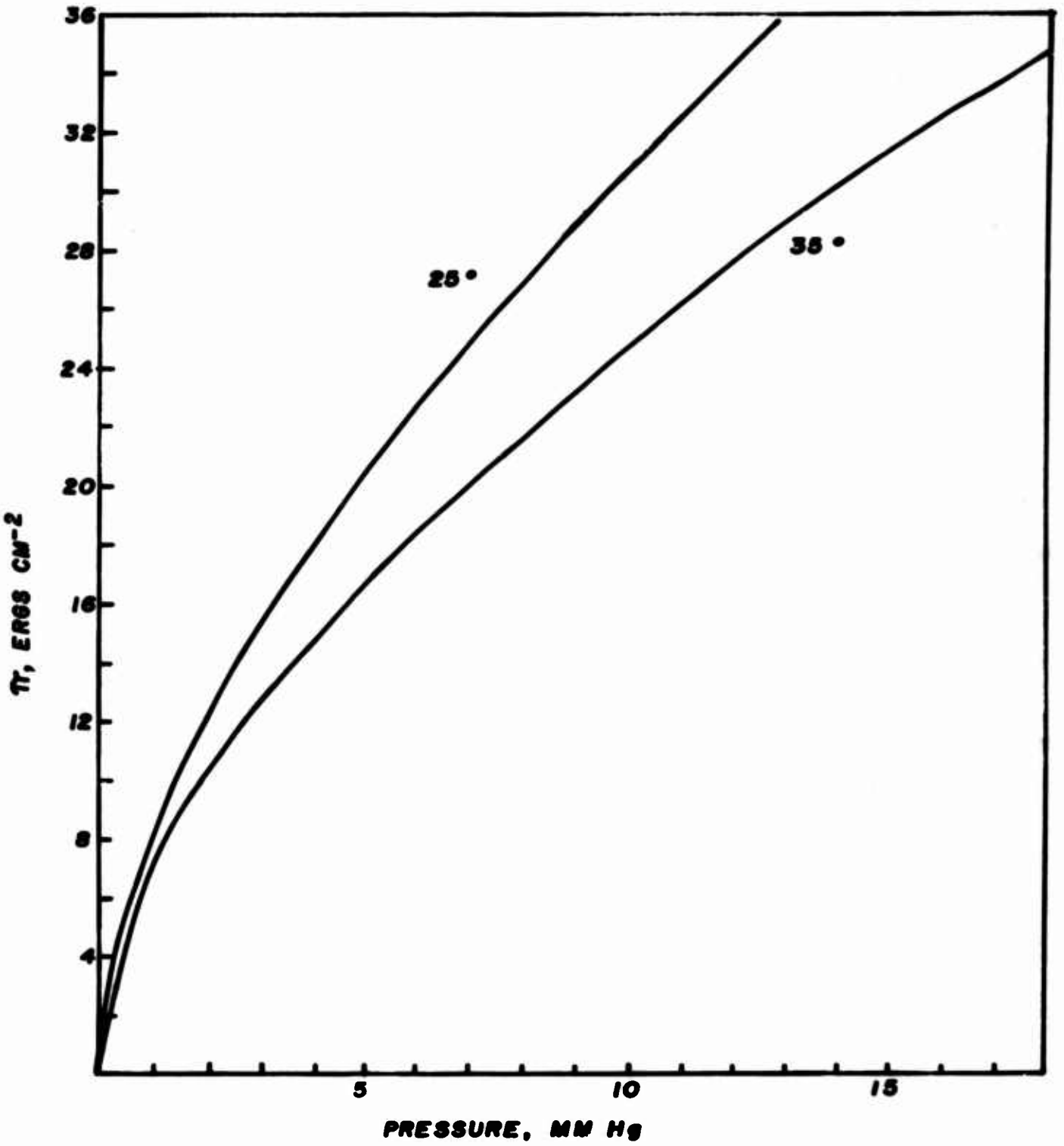

Fig 8 Variation of free surface energy of unground β-HMX by water at 25° and 35° vs pressure

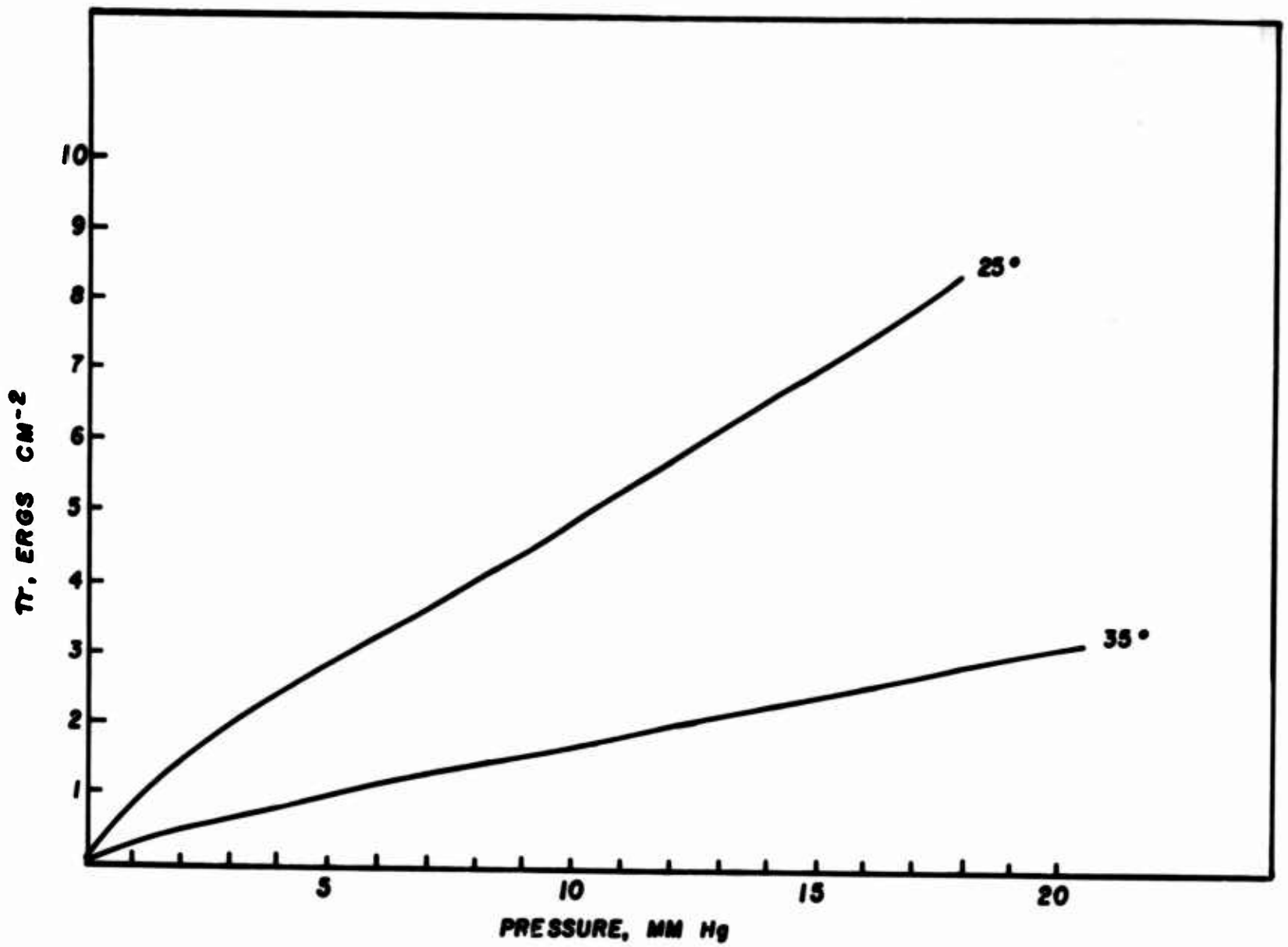

Fig 9 Variation of free surface energy of ground β-HMX by H_2O at 25° and 35° vs pressure

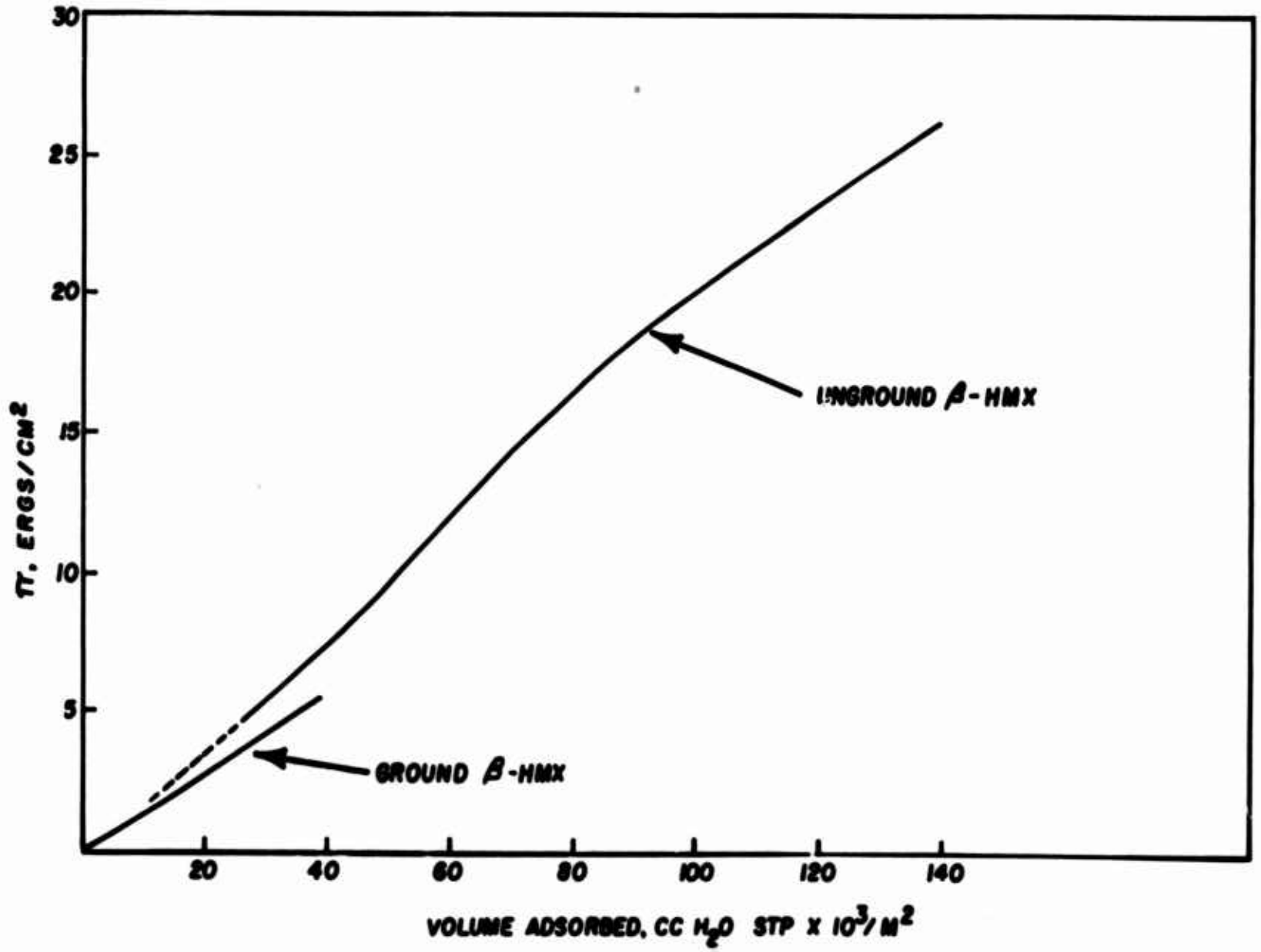

Fig 10 Lowering of free surface energy of ground and unground β-HMX by H_2O at 25° as a function of specific volume adsorbed

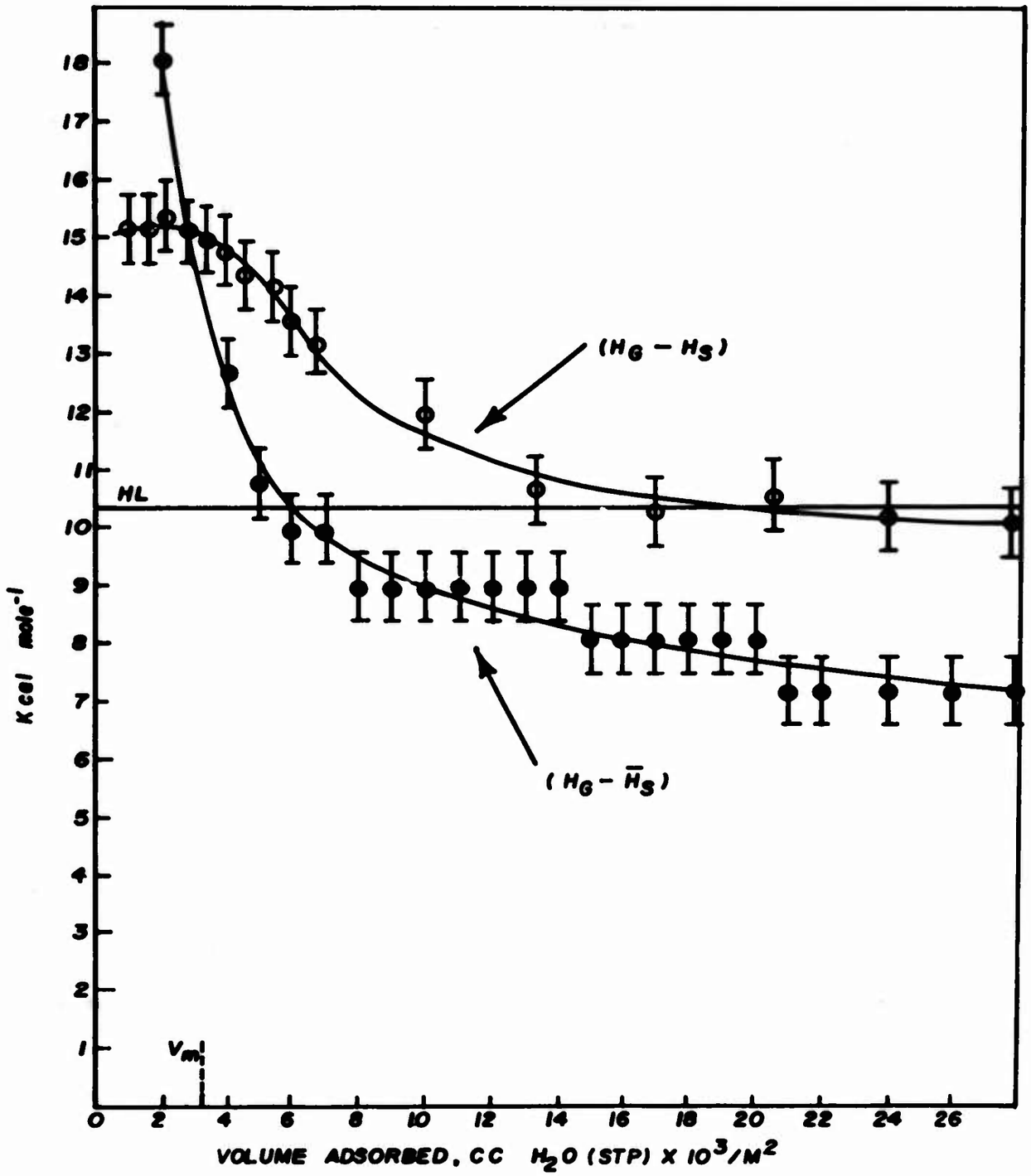

Fig 11 Isosteric and integral heats of water on ground β-HMX vs specific volume of adsorption

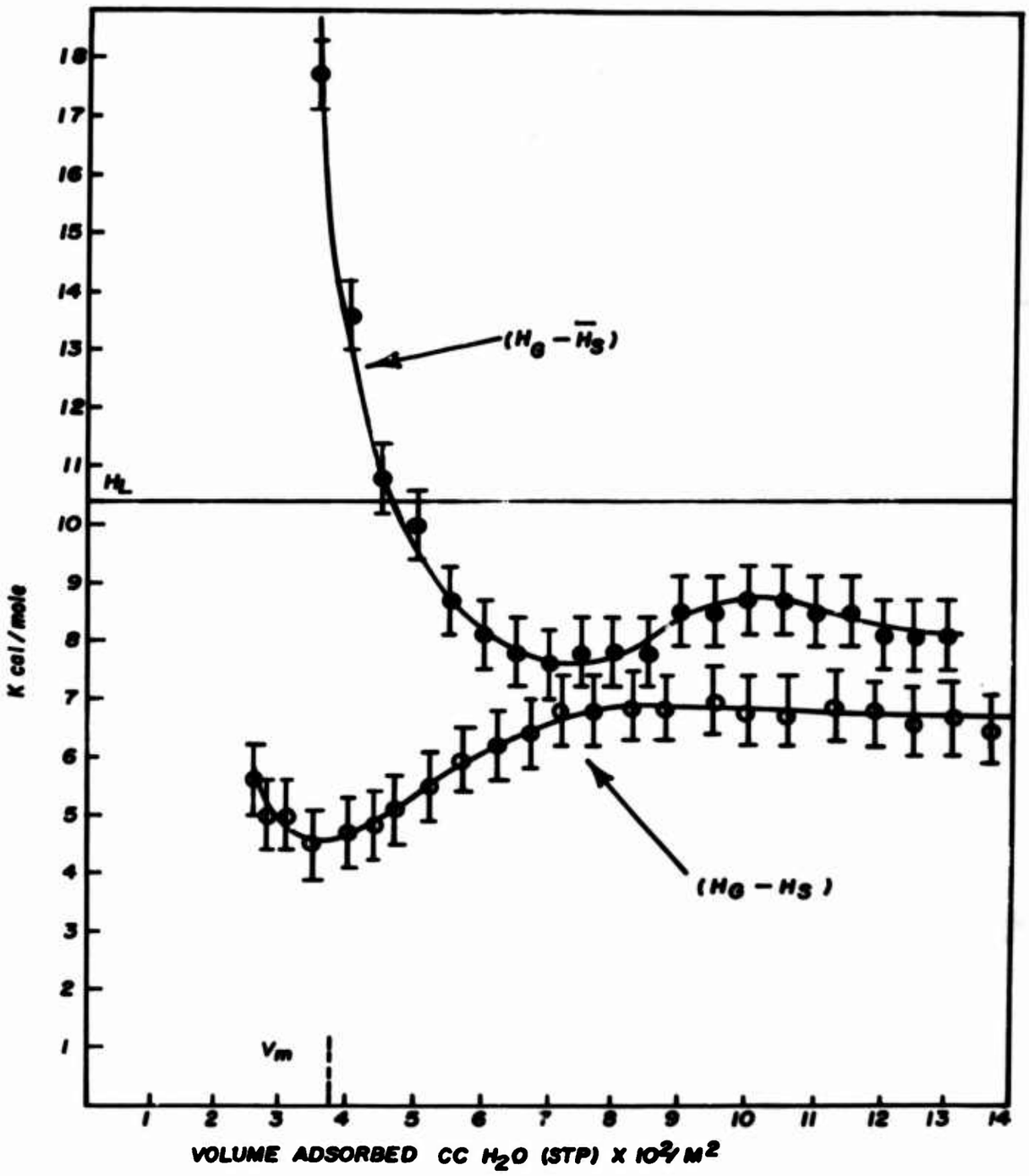

Fig 12 Isosteric and integral heats of water on unground β-HMX vs specific volume of adsorption

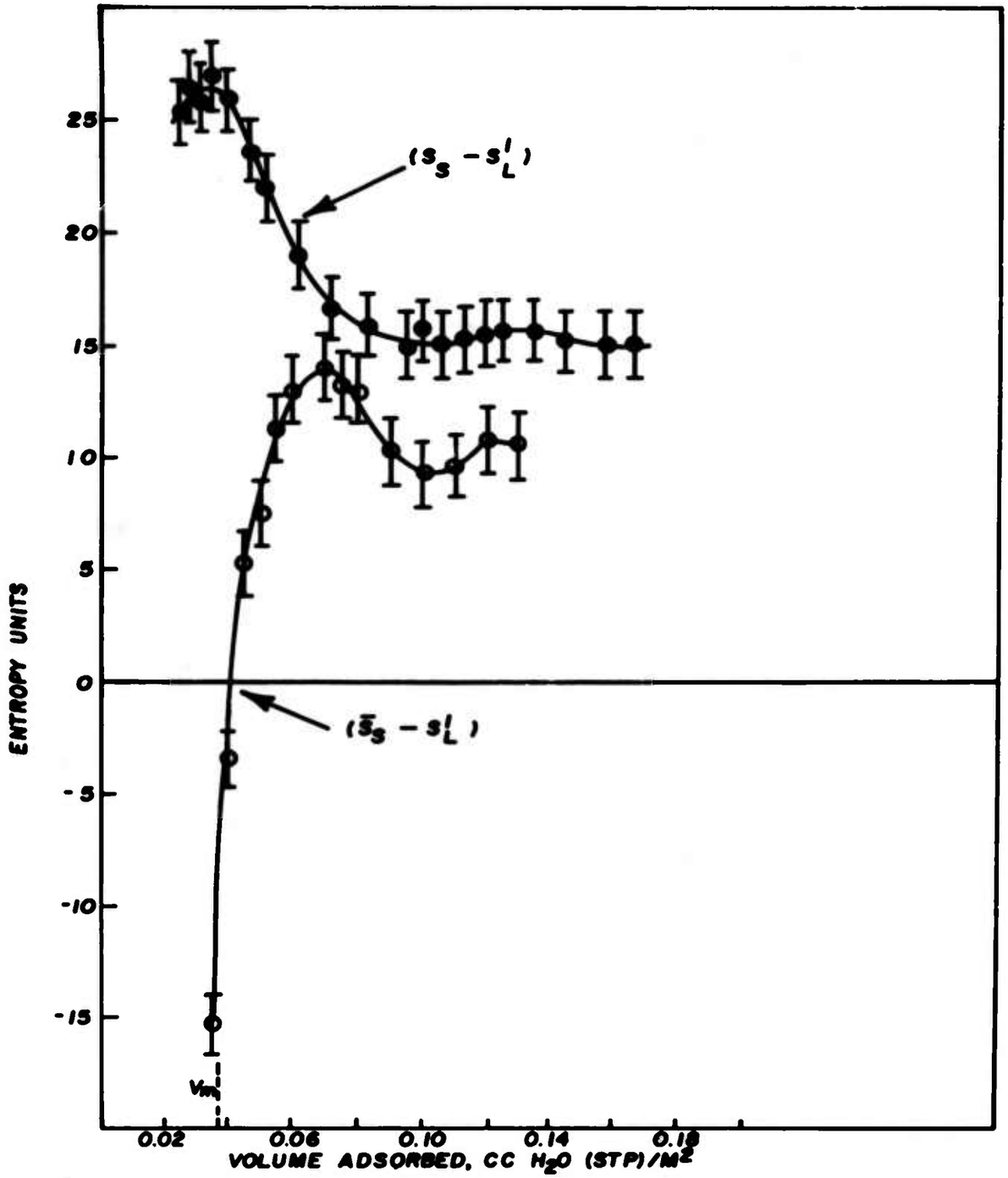

Fig 13 Differential and integral entropy changes of water on unground β-HMX vs specific volume of adsorption

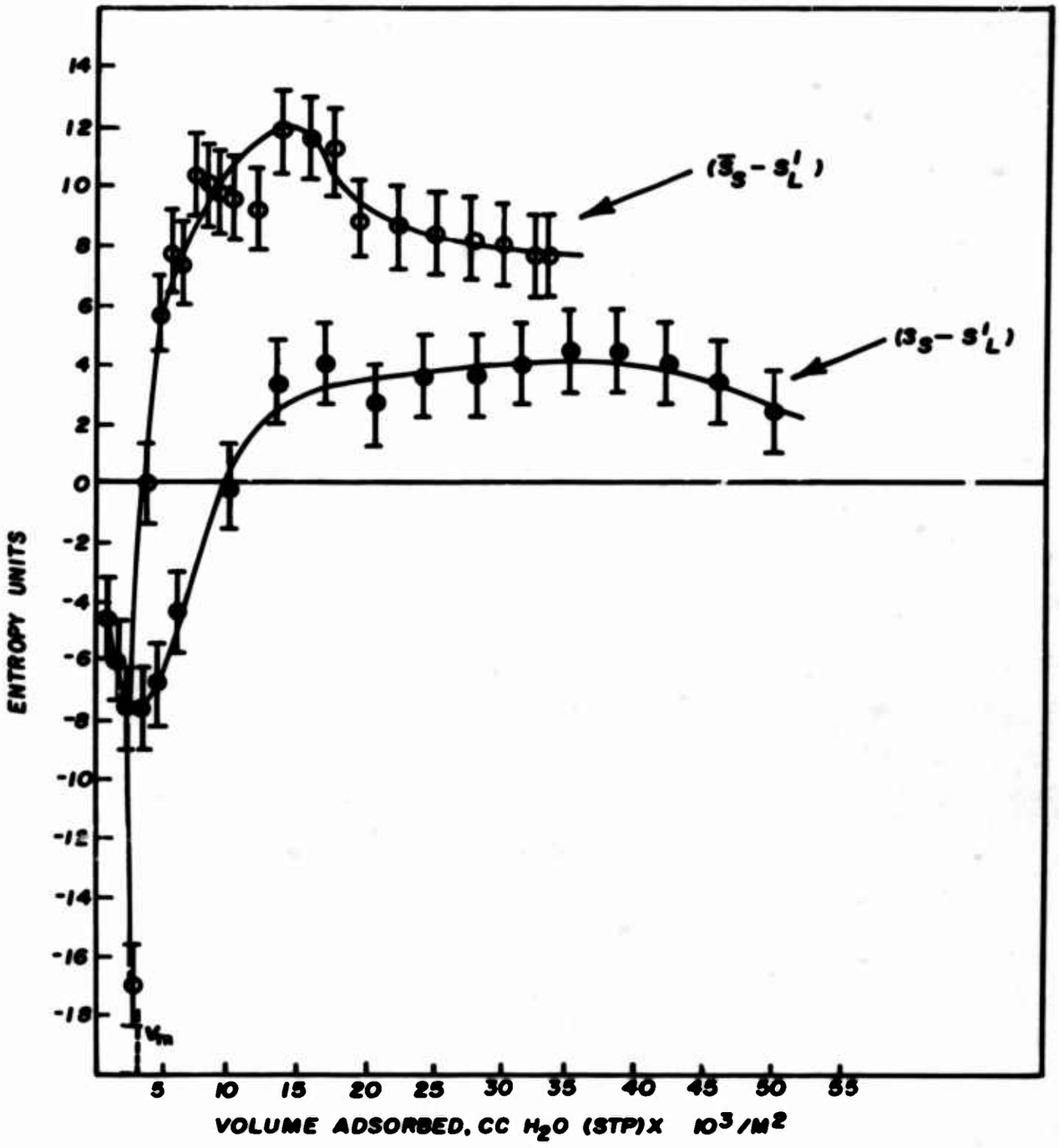

Fig 14 Differential and integral entropy changes of water on ground β-HMX vs specific volume of adsorption

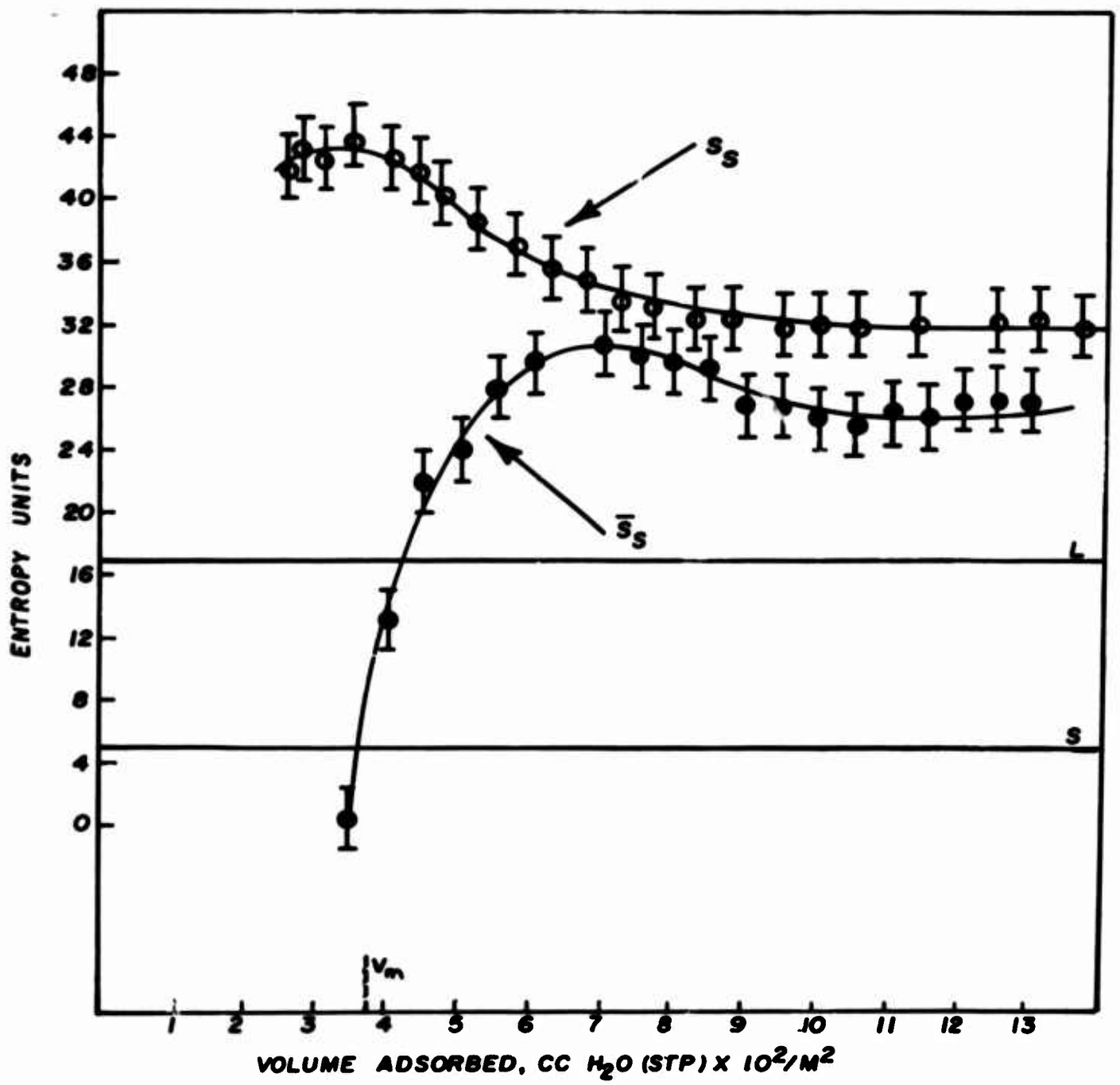

Fig 15 Differential and integral entropies of water on unground β-HMX vs specific volume of adsorption

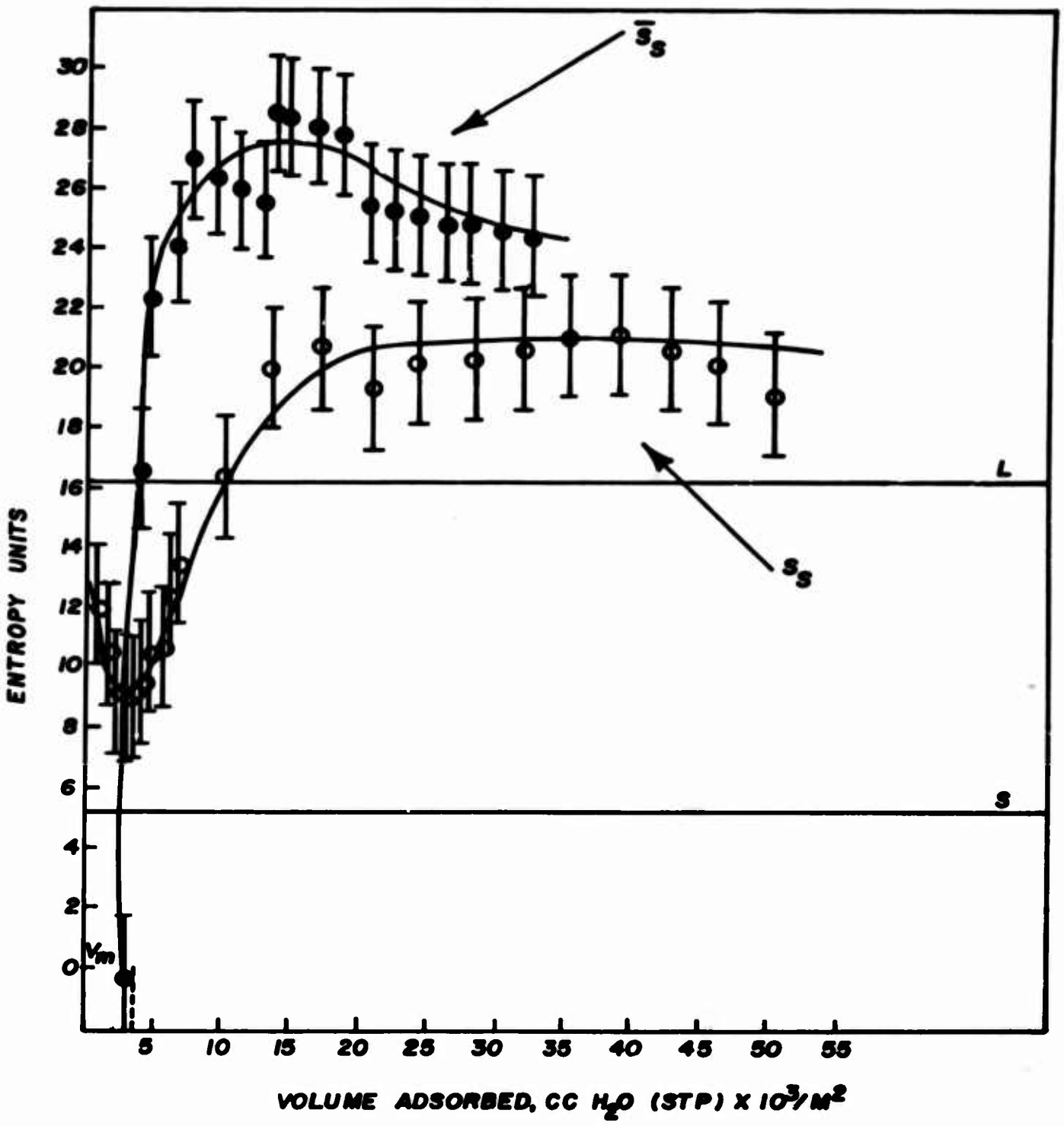

Fig 16 Differential and integral entropies of water on ground β-HMX vs specific volume of adsorption

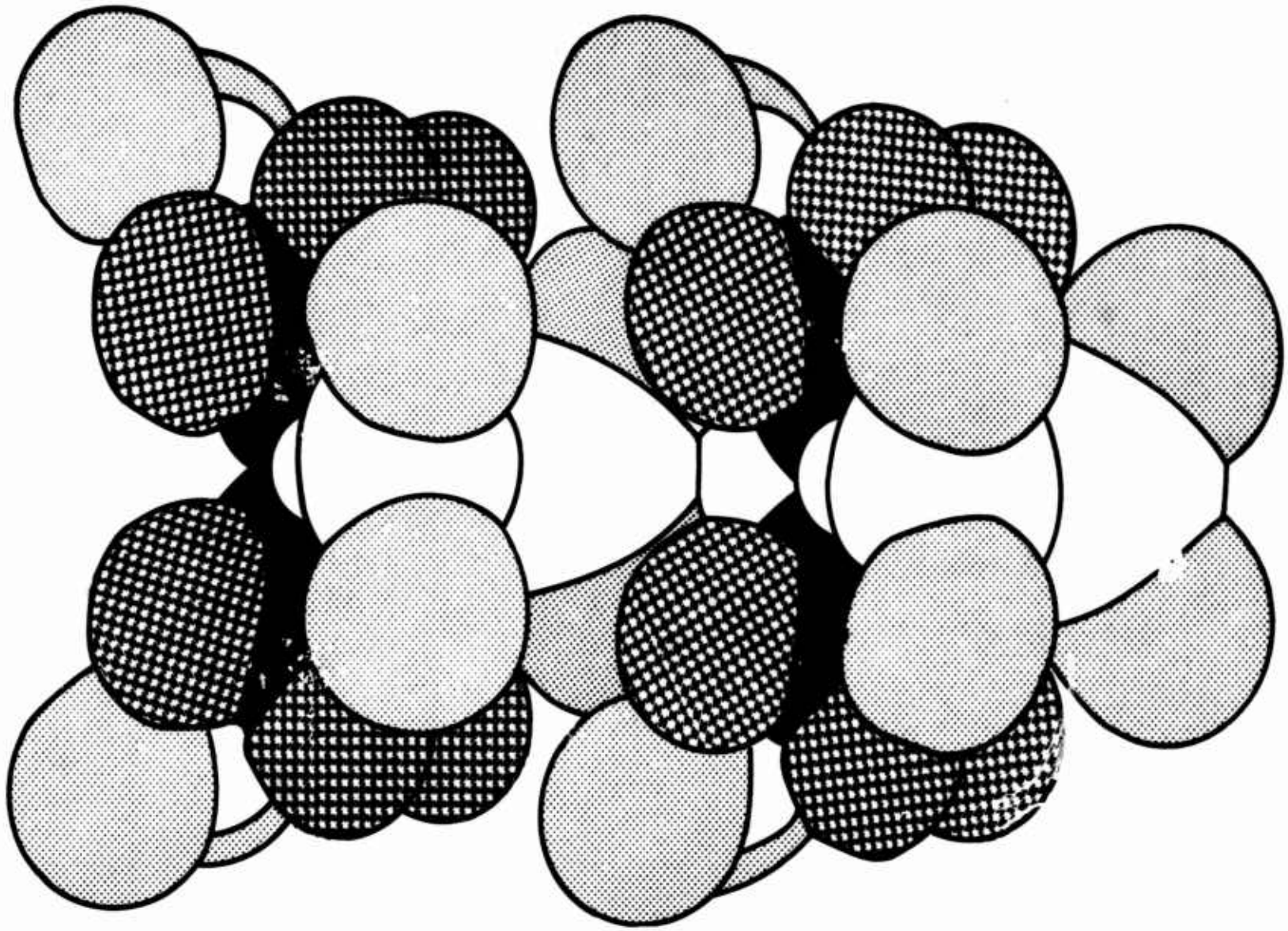

Fig 17 Fisher model of a unit cell of β-HMX showing free and methylene-shielded NO_2 groups (fine shading = oxygen; heavy shading = hydrogen; white = amino and nitro nitrogens; black = carbon)

UNCLASSIFIED
Security Classification

DOCUMENT CONTROL DATA - R & D

(Security classification of title, body of abstract and indexing annotation must be entered when the overall report is classified)

1. ORIGINATING ACTIVITY *(Corporate author)* Picatinny Arsenal, Dover, N. J. 07801	2a. REPORT SECURITY CLASSIFICATION Unclassified 2b. GROUP

3. REPORT TITLE
THE WATER ADSORPTION PROPERTIES OF THE POLYMORPHS OF HMX: THE THERMODYNAMICS OF WATER INTERACTION WITH GROUND AND UNGROUND BETA–HMX

4. DESCRIPTIVE NOTES *(Type of report and inclusive dates)*

5. AUTHOR(S) *(First name, middle initial, last name)*
Thomas C. Castorina, Jerome Haberman

6. REPORT DATE May 1967	7a. TOTAL NO. OF PAGES 36	7b. NO. OF REFS 15
8a. CONTRACT OR GRANT NO. b. PROJECT NO. DA Project 1L013001A91A c. AMCMS Code 5016.11.844 d.	9a. ORIGINATOR'S REPORT NUMBER(S) Technical Report 3555 9b. OTHER REPORT NO(S) *(Any other numbers that may be assigned this report)*	

10. DISTRIBUTION STATEMENT
Distribution of this document is unlimited

11. SUPPLEMENTARY NOTES	12. SPONSORING MILITARY ACTIVITY

13. ABSTRACT
Water adsorption isotherms were measured for the polymorphs of octahydro-1,3,5,7-tetranitro-s-tetrazine (HMX). Water is found to sorb into the crystal structure in the order, gamma-HMX > alpha-HMX, and not at all into beta-HMX. The thermodynamics of water interaction with the surface of beta-HMX was studied as a function of grinding action. Grinding reduces the free surface energy of beta-HMX from 25 to 5 ergs/sq cm, and increases the hydrophobic character of the surface by a factor of 12. The calculated thermodynamic functions support the concept of adsorption of water in clusters on both ground and unground beta-HMX surfaces. The integral heat of water adsorption increases with increasing hydrophobicity. This is attributed to unhindered dipole interaction of water with the more isolated active sites of like charges. Accordingly, water is shown to become less entropic as the hydrophobicity is increased.

DD FORM 1 NOV 65 1473 REPLACES DD FORM 1473, 1 JAN 64, WHICH IS OBSOLETE FOR ARMY USE.

UNCLASSIFIED
Security Classification

UNCLASSIFIED
Security Classification

14. KEY WORDS	LINK A ROLE	LINK A WT	LINK B ROLE	LINK B WT	LINK C ROLE	LINK C WT
Water adsorption isotherms						
Polymorphs of HMX						
Ground vs unground beta-HMX						
Free surface energy						
Hydrophobicity						
Thermodynamic functions (calculated)						
Integral heat of water adsorption						
Hydrophilic heterogeneities						
Polar sites						
Particle size						
Isosteric heats of adsorption						
Entropy						
Nitrogen adsorption						
Argon adsorption						

UNCLASSIFIED
Security Classification